# Preparation and characterization of uniform, spherical particles of $Y_2O_2S$ and $Y_2O_2S$:Eu

**Ligia Delgado da Vila, Elizabeth Berwerth Stucchi* and Marian Rosaly Davolos**

*Departamento de Química Geral e Inorgânica, Instituto de Química, Universidade Estadual Paulista, C.P. 355, CEP 14801-970, Araraquara, SP, Brasil*

The preparation of spherical $Y_2O_2S$ and $Y_2O_2S$:Eu particles using a solid–gas reaction of monodispersed precursors with elemental sulfur vapor under an argon atmosphere has been investigated. The precursors, undoped and doped yttrium basic carbonates, are synthesized by aging a stock solution containing the respective cation chloride and urea at 82–84 °C. $Y_2O_2S$ and $Y_2O_2S$:Eu were characterized in terms of their composition, crystallinity and morphology by chemical analysis, X-ray powder diffraction (XRD), IR spectroscopy, and scanning electron microscopy (SEM). The Eu-doped oxysulfide was also characterized by atomic absorption spectrophotometry and luminescence spectroscopy. The spherical morphology of oxysulfide products and of basic carbonate precursors suggests a topotatic inter-relationship between both compounds.

Rare-earth oxysulfides have been known for a long time as excellent phosphor host materials. When activated with trivalent europium, $Y_2O_2S$ becomes an important red phosphor in color TV picture tubes[1] because it has high brightness, short decay time, and exhibits long-term stability in poly(vinyl alcohol). Recently, yttrium oxysulfide has attracted a great deal of attention because of its electroluminescent properties.[2]

In modern technology, the necessity of dispersed powders consisting of uniform particles in size and shape is widely recognized. For example, in ceramic manufacture, there is a significant reduction in the sintering time and temperature if monodispersed powders are used as starting materials.[3] Phosphors used in both CRT and X-ray screens with uniform size distribution of the particles results in the best screen surfaces.[4] In materials science, the particle shape is equally important. Spherical morphology is interesting because most theoretical models dealing with fine particle properties and interactions are based on spherical particles. Furthermore, the size distribution of relatively uniform spherical particles can be determined by optical techniques without altering or destroying the system.[5]

Several methods are known for the preparation of rare-earth oxysulfides.[6] However, it seems that few investigations have been reported in the literature on spherical particle preparation of these phases. In a previous paper Luiz *et al.*[7] described the preparation process of lanthanum and yttrium oxysulfide powders by using a solid–gas reaction of oxalates with elemental sulfur vapor under an argon atmosphere. This paper reports an analogous method, using monodispersed basic carbonates as precursors. The present method is very attractive because the particle morphology of oxysulfide reproduces that of the basic carbonates. This fact indicates a topotatic inter-relationship between both groups of compounds. Thus, desired morphology for the oxysulfides can be achieved through the morphological control of precursor particles.

## Experimental

### Synthesis of doped and undoped yttrium oxysulfides

Yttrium and europium oxides (99.99 and 99.999% pure, Aldrich) were used as starting materials. Other chemicals used were grade reagents. Monodispersed yttrium basic carbonate particles were produced by heating a stock solution containing a cationic chloride and urea at 82–84 °C under continuous stirring for 2 h. This procedure, based on work by Matijevic and Hsu[8] and Sordelet and Akinc[9] was adapted by Santos.[10] Sulfidization of the basic carbonate precursor compounds was carried out in a horizontal tube furnace following the procedure outlined by Luiz.[7] Precursors were loaded into the principal furnace in an alumina crucible. The furnace was completely sealed to ensure an oxygen-free atmosphere. Argon gas was flushed through the system during both the reaction and cooling time. Sulfur was heated at 220 °C in an auxiliary furnace. Then the main furnace temperature was gradually increased to 770 °C (heating rate 2 °C $min^{-1}$) and sulfur vapor was carried by the argon stream across the system (flow rate 116 $cm^3$ $min^{-1}$). The end of the reaction was accompanied by bubbling of acid vapor products in alkaline solution until it reached constant pH. After the desired reaction time the auxiliary furnace was shut off and the product was heated at 800 °C for at least 2 h. The choice of synthesis temperature was based on DTA curve data.

### Characterization

Lanthanide content was assayed by EDTA titration using xylene orange as indicator. Atomic absorption spectrophotometry was performed using an INTERLAB AA-1475 atomic absorption spectrophotometer. X-Ray powder diffractograms were recorded on an XRD HZG-4B diffractometer equipped with Cu-K$\alpha$ or Co-K$\alpha$ radiation (36 kV, 20 mA). IR spectra in KBr pellets and Nujol in CsI windows were measured with Nicolet FT-730 and Impact 400 FTIR spectrometers. The particle morphology was examined in a scanning electron microscope JEOL-JSM-T330 A. Powders were pre-coated with Au using a cathodic sputtering Edwards S 150 B instrument. Emission spectra of Eu-doped oxysulfide were obtained in a Fluorolog Spex 212 I fluorescence spectrometer equipped with an R928 Hammamatsu photomultiplier. The samples were excited by a 450 W xenon lamp.

## Results and Discussion

### EDTA titration and atomic absorption spectrophotometry

EDTA titration and atomic absorption spectrophotometry results of the oxysulfides are shown in Table 1. As can be seen, the agreement between calculated and obtained results are satisfactory.

**Table 1** EDTA titration and atomic absorption spectrophotometry results for yttrium oxysufide particles

| | Ln (mass%) | | | |
|---|---|---|---|---|
| | EDTA titration | | atomic absorption spectrophotometry | |
| compound | found | calc. | found | calc. |
| $Y_2O_2S$ | 73.97 | 73.52 | — | — |
| $(Y_{0.964}Eu_{0.036})_2O_2S$ | 75.30 | 74.00 | 4.26 | 4.44 |

## X-Ray diffraction

The $d_{hkl}$ data of the oxysulfides are shown in Table 2. The precursors were non-crystalline and the products of their thermodecomposition under sulfur and Ar atmosphere yielded an X-ray pattern identified as crystalline $Y_2O_2S$.[11] The results did not exhibit patterns due to oxysulfate and/or oxide phases in the oxysulfide samples.

## FTIR spectroscopy

IR spectra of $Y_2O_2S$ and $Y_2O_2S$:Eu, obtained between 4000 and 400 $cm^{-1}$ (high-frequency region) and 1500 to 220 $cm^{-1}$ (low-frequency region) are shown in Fig. 1 and 2, respectively. In the high-frequency region, the absence of the S—O stretching band at 1200 $cm^{-1}$ attributed to sulfate,[12] is noted. This suggests that the oxygen was entirely removed from the reaction system. Moreover, the bands corresponding to the carbonate group were also missing, suggesting the absence of precursor. In the low-frequency region, absorptions in the range 800–220 $cm^{-1}$ can be attributed to Ln—O or Ln—S vibrations. This assignment is very difficult because of the proximity of the bands. However, if this sample spectrum is compared with that of yttrium oxide (Fig. 3), oxysulfide phase formation is evidenced. The oxysulfide spectrum exhibits less broad and strong bands than those observed for the oxide (see Table 3). This behavior could be understood considering that

**Table 2** X-Ray diffraction powder data for yttrium oxysulfide

| lit.[11] | | this work | | | |
|---|---|---|---|---|---|
| | | $Y_2O_2S$ | | $Y_2O_2S$:Eu | |
| $d$/Å | $I/I_o$(%) | $d$/Å | $I/I_o$(%) | $d$/Å | $I/I_o$(%) |
| 3.280 | 35 | 3.255 | 31 | 3.283 | 32 |
| 2.930 | 100 | 2.942 | 100 | 2.920 | 100 |
| 2.320 | 60 | 2.320 | 40 | 2.312 | 34 |
| 2.190 | 16 | — | — | — | — |
| 1.892 | 65 | 1.885 | 38 | 1.889 | 34 |
| 1.824 | 45 | 1.817 | 23 | 1.819 | 32 |
| 1.642 | 30 | 1.639 | 16 | 1.640 | 16 |
| 1.591 | 25 | 1.587 | 18 | 1.589 | 15 |

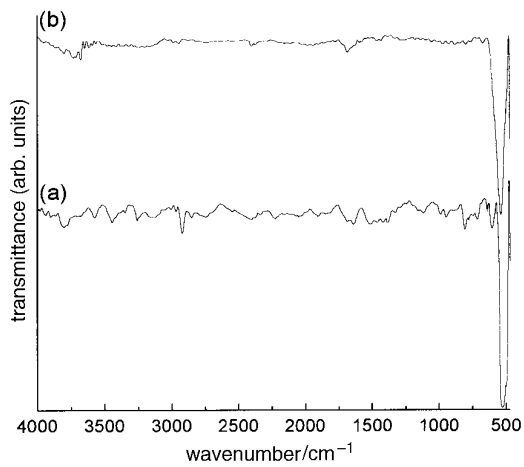


**Fig. 1** FTIR spectra for yttrium oxysulfides in KBr pellets (4000 to 400 $cm^{-1}$ range): (a) yttrium oxysulfide; (b) Eu-doped yttrium oxysulfide

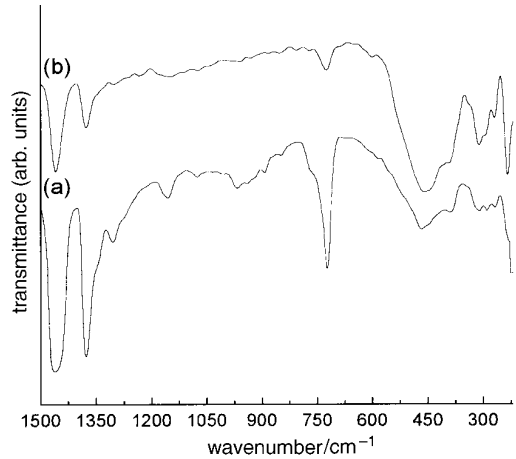


**Fig. 2** FTIR spectra for yttrium oxysulfides in Nujol–CsI windows (1500 to 220 $cm^{-1}$ range): (a) yttrium oxysulfide; (b) Eu-doped yttrium oxysulfide

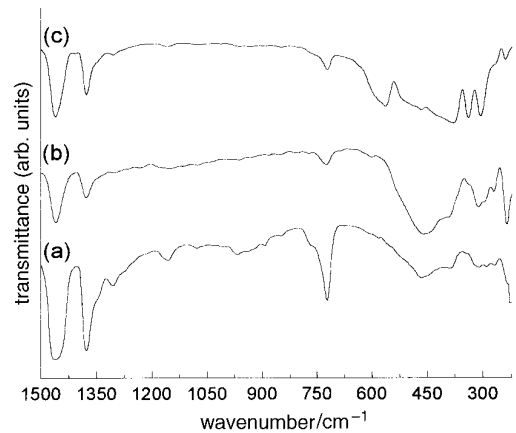


**Fig. 3** FTIR obtained in Nujol–CsI windows (1500 to 220 $cm^{-1}$ range): (a) yttrium oxysulfide; (b) Eu-doped yttrium oxysulfide; (c) yttrium oxide

**Table 3** Comparative frequency ranges of yttrium oxysulfide, Eu-doped yttrium oxysulfide and yttrium oxide bands

| wavenumber/cm$^{-1}$ | | |
|---|---|---|
| $Y_2O_2S$ | $Y_2O_2S$:Eu | $Y_2O_3$ |
| — | 235m (sp) | 238w (sp) |
| 269m (sh)[a] | 270w (sh) | 270w (sh) |
| 290m (sh) | — | — |
| — | — | 306s (sp) |
| 310m (sh) | 312m (sh) | — |
| — | — | 339s (sp) |
| 391m (sh) | 394m (sh) | 380s (br) |
| 467s (br) | 462s (br) | 466s (sp) |
| — | — | 563s (br) |

[a]Band features: br = broad, sp = sharp; sh = shoulder. Band intensity; s = strong, m = medium, w = weak.

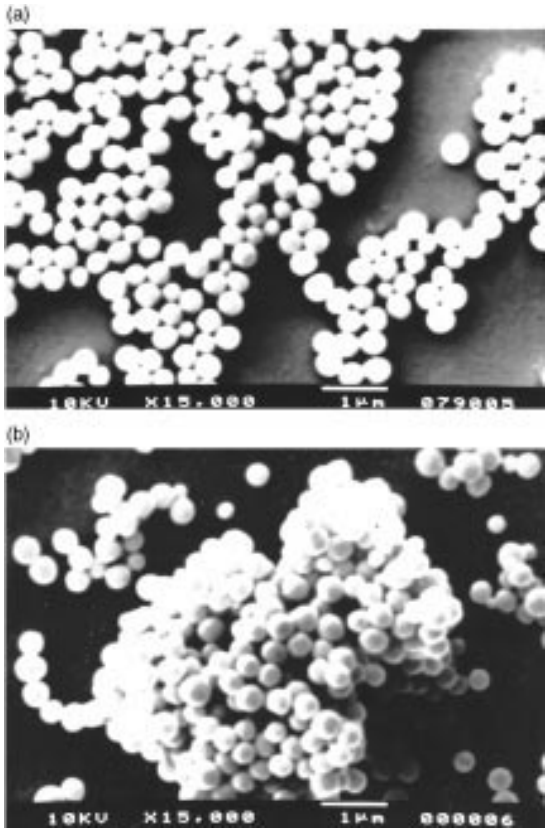


**Fig. 4** Electron micrographs of: (a) yttrium basic carbonate; (b) yttrium oxysulfide

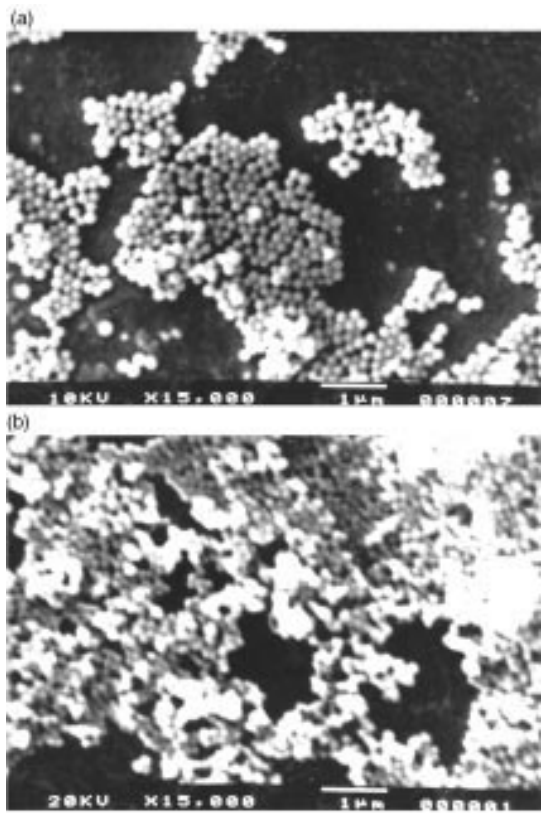


**Fig. 5** Electron micrographs of: (a) Eu-doped yttrium basic carbonate; (b) Eu-doped yttrium oxysulfide

there are only contributions from $C_{3v}$ symmetry for $Y_2O_2S$,[13] while in $Y_2O_3$ there are contributions from $C_{2v}$ and $S_6$ symmetry.[14] Therefore, the IR spectra suggest that the Ln—S vibrations are present. This result corroborates the XRD data, showing the formation of the oxysulfide phase. The absorptions at 1460, 1376 and 723 $cm^{-1}$ are characteristic of Nujol vibrational modes.

### Scanning electron microscopy

Scanning electron micrographs of the basic carbonate precursors and oxysulfides are shown in Fig. 4 and 5, respectively. The precursor and oxysulfide particles were relatively uniform in size and spherical in shape. The average particle size of both undoped basic carbonates and oxysulfides was 0.4 μm, while Eu-doped precursors and oxysulfides showed a medium particle size of 0.2 μm. This suggests that the dopant can influence the size of the particles, but further study is required to confirm this effect. Fig. 4(b) and 5(b) show that no change in morphology took place during the sulfidization procedure. This suggests the occurrence of a topotatic reaction from basic carbonates to oxysulfides. It can be observed that slight sintering occurs during thermal processing of the precursors.

### Luminescence spectroscopy

Emission spectra of Eu-doped oxysulfide obtained at room temperature ($\lambda_{exc}=311$ nm) and 77 K ($\lambda_{exc}=303$ nm) are shown in Fig. 6(a) and (b), respectively. The main signals are found in the region between 580 and 630 nm. The assignments agree

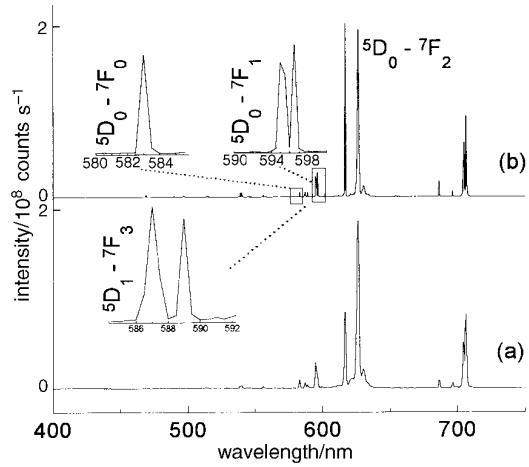


**Fig. 6** Emission spectra of Eu-doped yttrium oxysulfide (400–750 nm range): (a) room temperature ($\lambda_{exc}=311$ nm); (b) 77 K ($\lambda_{exc}=303$ nm)

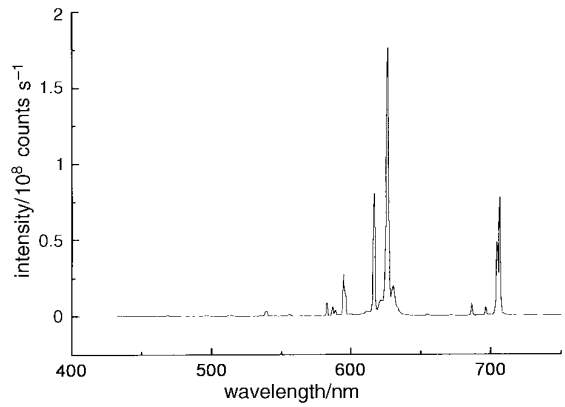


**Fig. 7** Emission spectra of Eu-doped yttrium oxysulfide (400–750 nm range, room temperature, $\lambda_{exc}=265.5$ nm)

with that expected for $C_{3v}$ symmetry.[13] The dominant emission arises from the $^5D_0 \rightarrow {}^7F_2$ transition and is observed at 626 nm. According to crystal-field theory, the $J=0$ state does not split ($A_1$), and the $J=1$ state splits into two Stark levels ($A_2$ and E) resulting in one and two emission bands, respectively. This observed behavior indicates only one emitting $Eu^{3+}$ symmetry site. The emission spectrum obtained at 265.5 nm excitation, characteristic of $Eu^{3+}$ in yttrium oxide, is shown in Fig. 7. No peak arising from a $^5D_0 \rightarrow {}^7F_2$ transition at 611 nm is observed, suggesting the absence of oxide impurity.

The authors would like to thank to CNPq for a scholarship (L.D.V.).

## References


1 P. N. Yocom, *US Pat*., 3 418 247, 1968.
2 (*a*) K. Sowa, M. Tanabe, S. Furukawa, Y. Nakanishi and Y. Hatanaka, *Electroluminescence, Proc. Int. Workshop 6th*, 1992, p. 315; (*b*) K. Sowa, M. Tanabe, S. Furukawa, Y. Nakanishi and Y. Hatanaka, *Jpn. Appl. Phys*., 1993, **32**, 12A, 5601.
3 Y. Her, E. Matijevic and W. R. Wilcox, *J. Mater. Sci. Lett*., 1992, **11**, 1629.
4 L. H. Brixner, *Mater. Chem. Phys*., 1987, **16**, 253.
5 (*a*) E. Matijevic, *CHEMTECH*, 1991, **21**, 176; (*b*) E. Matijevic, *Annu. Rev. Mater. Sci*., 1985, **15**, 483.
6 (*a*) M. Leskelä, *Res. Pap*., 1980, **64**, 39; (*b*) O. Kanehisa, T. Kano and H. Yamamoto, *J. Electrochem. Soc*., 1985, **132**, 2023.
7 J. M. Luiz, E. B. Stucchi and N. Barelli, *Eur. J. Solid State Inorg. Chem*., 1996, **33**, 321.
8 E. Matijevic and W. P. Hsu, *J. Colloid Interface Sci*., 1987, **118**, 506.
9 D. Sordelet and M. Akinc, *J. Colloid Interface Sci*., 1987, **122**, 47.
10 M. F. Santos, *Estudo de Precursores para Materiais Luminescentes: Hidroxicarbonatos de ítrio e de Gadolínio Dopados*, M. Sc. Dissertation, Instituto de Química, UNESP, Araraquara, 1993.
11 JCPDS 24-1424.
12 J. R. Ferraro, *Low-Frequency Vibrations of Inorganic and Coordination Compounds*, Plenum Press, New York, 1971.
13 O. J. Sovers, T. Yoshioka, *J. Chem. Phys*., 1968, **49**, 4945.
14 H. Forest, G. Ban, *J. Electrochem. Soc*., 1969, **116**, 474.


*Paper* 7/01540B; *Received* 4*th March*, 1997